EARTH SURFACE PROCESSES AND LANDFORMS
Earth Surf. Process. Landforms **41**, 526–542 (2016)

Published online 5 November 2015 in Wiley Online Library
(wileyonlinelibrary.com) DOI: 10.1002/esp.3846

Morphodynamic evolution of a lower Mississippi River channel bar after sand mining

Brendan T. Yuill,[1]* Ahmed Gaweesh,[2] Mead A. Allison[1,3] and Ehab A. Meselhe[1]
[1] The Water Institute of the Gulf, Baton Rouge, LA, USA
[2] Pontchartrain Institute of Environmental Sciences, The University of New Orleans, New Orleans, LA, USA
[3] Department of Earth and Environmental Studies, Tulane University, New Orleans, LA, USA

Received 31 December 2014; Revised 17 September 2015; Accepted 29 September 2015

*Correspondence to: Brendan T. Yuill, The Water Institute of the Gulf, Baton Rouge, LA, 70825, USA. E-mail: brendan.yuill@gmail.com

ESPL
Earth Surface Processes and Landforms

ABSTRACT: In-channel sand mining by dredge removes large quantities of bed sediment and alters channel morphodynamic processes. While the reach-scale impacts of dredging are well documented, the effects of the dredged borrow pit on the local flow and sediment transport are poorly understood. These local effects are important because they control the post-dredge evolution of the borrow pit, setting the pit lifespan and affecting reach-scale channel morphology. This study documents the observed morphological evolution of a large (1·46 million m^3) borrow pit mined on a lateral sandbar in the lower Mississippi River using a time-series of multibeam bathymetric surveys. During the 2·5 year time-series, 53% of the initial pit volume infilled with sediment, decreasing pit depth by an average of 0·88 m yr^{-1}. To explore the controls of the observed infilling, a morphodynamic model (Delft3D) was used to simulate flow and sediment transport within the affected river reach. The model indicated that infilling rates were primarily related to the riverine sediment supply and pit geometry. The pit depth and length influenced the predicted magnitude of the pit bed shear stress relative to its pre-dredged value, i.e. the bed-stress reduction ratio (R^*), a metric that was correlated with the magnitude and spatial distribution of infilling. A one-dimensional reduced-complexity model was derived using predicted sediment supply and R^* to simulate patterns of pit infilling. This simplified model of borrow-pit evolution was able to closely approximate the amount and patterns of sediment deposition during the study period. Additional model experiments indicate that, for a borrow pit of a set volume, creating deep, longitudinally-shorter borrow pits significantly increased infilling rates relative to elongated pits. Study results provide insight into the resilience of alluvial river channels after a disturbance and the sustainability of sand mining as a sediment source for coastal restoration. Copyright © 2015 John Wiley & Sons, Ltd.

KEYWORDS: sand mining; sand bed rivers; channel evolution modeling; Delft3D; Mississippi River

Introduction

Sand mining in alluvial rivers by hydraulic or bucket dredge causes a disturbance within the geomorphic processes controlling the river form and function (Kondolf, 1997; Meador and Layher, 1998). Dredging removes a significant volume of sediment, typically from a channel bar, creating a large, steep-walled excavation pit within the channel bed. The excavation pit, commonly referred to as a 'borrow pit', directly impacts the sediment transport regime by reducing the local supply of bed sediment available for transport downstream. A wealth of past research (e.g. Bull and Scott, 1974; Collins and Dunne, 1989; Petit *et al.*, 1996; Mossa and McLean, 1997, Rinaldi and Simon, 1998; Marston *et al.*, 2003; Lou *et al.*, 2007; Padmalal *et al.*, 2008; Wishart *et al.*, 2008; Kori and Mathada, 2012) indicates that this reduction in sediment supply may have a profound influence on the river channel character during the lifespan of the pit, leading to deflation within the proximal channel bar as well as bed incision and textural coarsening further downstream. An additional impact of the borrow pit is that it alters the hydraulic properties of the flow (e.g. velocities and shear stress) as the flow approaches, enters, and exits the affected area of the channel bed (van Rijn, 1986; Chang, 1987; Chen, 2011). One of the primary effects of this altered hydraulic environment is the net reduction in sediment transport capacity which leads to an increase in sediment deposition within the borrow pit, reducing the time it takes to 'heal' the disturbance to the system (Simon, 1989; van Rijn and Walstra, 2002). While the rate at which the infilling occurs is an important variable because it sets the lifespan of the pit and its impact on the fluvial system, little is known about its controls in rivers. Theoretically, the borrow-pit infilling rate would be dependent on the supply of sediment to the borrow pit and the reduction of the fluvial forces within the borrow pit that leads to sediment deposition (van Rijn, 1986); however, the nature of these dependences has not been well quantified into a coherent relationship using field observational data in rivers.

In addition to instream mining, other anthropogenic activities require the excavation of sediment from alluvial channel beds and may result in the formation of borrow pit-type landforms and impacts (Watson *et al.*, 1999). For example, dredging bed sediment to deepen channels for improved navigation (e.g. Hossain *et al.*, 2004; Ohimain

2004) and flood control (e.g. Bird, 1980; Griggs and Paris, 1982; Bai *et al.*, 2003) may result in elongated or diffuse excavation pits that decouple the river channel morphology from the river's ability to transport its typical load of flow and sediment in much the same manner as instream mining. Despite the increased occurrence of these activities in major waterways worldwide over the last few decades (IADC/IAPH, 2010; USACE, 2015), a survey of published literature suggests that case studies of the local geomorphic response to these activities are rare.

This paper reports the results of an investigation on the relationship between sediment supply, borrow-pit flow hydrodynamics, and borrow-pit infilling within a lower Mississippi River (LMR) channel bar in Louisiana, USA using both field-based and numerical methods. An improved understanding of infilling patterns and rates enhances the ability of river engineers and managers to predictively model how a river channel bar will respond to mining-related disturbances and to schedule future dredging accordingly (van Rijn and Walstra, 2002). This ability also has theoretical implications, offering insight on river-system resilience to morphodynamic disturbances analogous to extreme natural events that cause a sudden, high-intensity reduction in sediment supply such as the formation of a debris (or ice, lava) dam or flood scour (e.g. Gupta and Fox, 1974; Keller and Swanson, 1979; Costa and Schuster, 1988; Grant and Swanson, 1995; Lapointe *et al.*, 1998; Smith and Pearce, 2002). Furthermore, accurate prediction of the persistence of a borrow pit through time allows resource managers to better assess the duration of its ecological impacts, such as altered current velocities and water quality (e.g. salinity, temperature, turbidity), which can adversely affect aquatic and benthic habitats (Saloman *et al.*, 1982; Meador and Layher, 1998; Rempel and Church, 2009).

This paper has three primary objectives. The first objective of this paper is to summarize and interpret field measurements of borrow-pit evolution. The second objective is to investigate how borrow-pit geometry affected the local river hydrodynamics and how, in turn, the hydrodynamics affected bed sediment (i.e. sand) transport and borrow-pit infilling. The third objective is to formalize the relationship between pit geometry, flow dynamics, and borrow-pit infilling into a one-dimensional reduced-complexity model that replicates the observed borrow-pit evolution.

Background

Sand mining in alluvial rivers

Alluvial river channels often contain large reserves of coarse sediment (i.e. sands and gravels) that have utility to many industries (e.g. commercial development, environmental restoration) as a construction material (Langer and Glanzman, 1993; Meador and Layher, 1998). These reserves are the product of natural fluvial suspended load and bedload sediment transport processes that concentrate a well-sorted, surficial and near-surficial sediment deposit. These deposits typically have significant monetary value to industry because of their accessibility and uniformity of material (Poulin *et al.*, 1994; Kondolf, 1997). The coarse sediment may be mined using a multitude of different methods (Langer, 2003); however, mechanical dredging is commonly employed to excavate sandy material from submerged regions of the river channel bed and bars. Dredging allows targeted removal of sediment from a borrow area while minimally disturbing the surrounding channel bed. The geometry of the resultant borrow pit is typically contingent on a priori conditions such as: (1) the volume of borrow material needed; (2) the method of extraction; (3) the thickness and extent of the coarse sediment deposit; (4) the potential impact of mining on nearby navigational channels or on river bank stability.

In rivers, our contemporary understanding of borrow-pit hydrodynamics and sedimentation is primarily limited due to a lack of comprehensive field observations which are difficult and costly to obtain; the majority of our knowledge on the subject is theoretical and has been developed from numerical and laboratory experiments (Kraus and Larson, 2001, 2002; van Rijn and Walstra, 2002; Bender and Dean, 2003). There are a small number of relevant field observational datasets in river channels (e.g. Owen *et al.*, 2012); however, the majority of field-based borrow-pit research tends to be in coastal areas that are significantly impacted by waves, tidal cycles, and multi-directional currents (e.g. Kojima *et al.*, 1986; Hoitink, 1997; Klein, 1999; Boers, 2005; González *et al.*, 2010; Van Lancker *et al.*, 2010) which reduces its application to riverine systems.

Fredsoe (1979), Bijker (1980), and Alfrink and van Rijn (1983) were among the first to derive theoretical models of borrow-pit morphodynamics. Their research identified two general driving phenomena: (1) the transition of the upstream channel into the borrow pit that increases the local river depth, reduces the near-bed flow velocities, and promotes fluvial sediment deposition and (2) the transition from the borrow pit to the downstream channel that contracts and accelerates flow, causing local bed sediment erosion. The net result of these phenomena cause downstream translation of the pit accompanied by gradual infilling in most environments; super-critical flow may initiate significant erosion at the channel edge upstream of the pit and cause net upstream translation (Ponce *et al.*, 1979).

Fredsoe (1979) predicted that borrow-pit infilling was predominately a result of bedload transport rather than suspended load transport. This was because the length-scales of typical dredged pits are small relative to the length-scale required for a significant fraction of the suspended sediment to settle out of the flow due to the reduction in flow velocity. More recent studies have sought to refine these theoretical models by testing the average effects of parameters such as borrow-pit geometry (Lee *et al.*, 1993; Jensen and Fredsøe, 2001; Roos *et al.*, 2008), the pit location within a channel (Neyshabouri *et al.*, 2002), and the pit orientation relative to dominant currents (van Rijn 1986; Jensen *et al.*, 1999).

Van Rijn and Tan (1985) developed a comprehensive computational model specifically designed to simulate sedimentation in submarine trenches (SUTRENCH) applicable to engineering problems; it predicts sediment deposition primarily as a function of sediment input, the approach velocity of the flow, and trench geometry. While functionally the model is applicable to riverine borrow pits, it has been predominantly validated-in and applied-to marine applications (Walstra *et al.*, 1998; Klein, 1999; Walstra *et al.*, 1999). Despite the breadth of information produced by the studies identified earlier, the relative absence of published research coupling field observations with quantitative analyses, especially on borrow pits in rivers, has limited further model development and application to real word predictions in fluvial environments.

Sand dredging in the lower Mississippi River (LMR)

The LMR below New Orleans, Louisiana has been increasingly used as a source of sand for coastal restoration projects over the last few decades as the magnitudes of the available sand within

the channel system have become apparent (Allison *et al.*, 2012; Allison *et al.*, 2014; Nittrouer and Viparelli, 2014). Recent surveys estimate that there is approximately 250 million m^3 of sand located in the large channel bars that punctuate the channel (Moffatt and Nichol 2012a). These channel bars are typically 10 to 30 m thick and consist of well-sorted fine and medium sands between 0·12 and 0·4 mm in diameter (Finkl *et al.*, 2006). The top 1 to 2 m of these bars consist of modern, seasonally mobile, deposits of fluvial bedload (Allison and Nittrouer, 2004) covered in dunes, while deeper material is likely relict sediment of similar texture.

As the LMR channel bars are increasingly exploited as borrow areas for a wide range of uses, resource managers have begun to examine their long-term sustainability (Khalil and Finkl, 2009). Sand mining is sustainable if the excavated sediment is recharged by new sediment supplied by upstream sources. Sustainable recharge requires that two provisions be met: (1) the sediment is, on average, not removed at rates faster than it can be replaced and (2) the new sediment has the same physical properties (e.g. grain size) as the original bar material. In coastal Louisiana the growing number of planned restoration projects in need of sandy borrow material (Peyronnin *et al.*, 2013), coupled with the fact there are no signs that the significant rates of land loss will naturally cease (e.g. Blum and Roberts, 2009), produce tremendous pressure to mine sand for marsh creation and barrier island restoration at the maximum-sustainable rate (Khalil and Finkl, 2009). The identification of this optimal rate of sand mining is difficult because there are few field studies illustrating how borrow pits evolve in rivers and there is a paucity of predictive models applicable to fluvial systems like the LMR. For example, past research provides little insight into what environmental variables control the rate at which a borrow pit would infill in a real world setting. Identifying these variables is vital to developing and managing sustainable sand mining activities.

Study Area

From November 2009 to March 2010, approximately 3 million m^3 of sediment was dredged from a ~1·0 km^2 LMR channel bar (Figure 1) to provide borrow material for the State of Louisiana's BA-39 Bayou Dupont marsh creation project (see Richardi *et al.*, 2013; http://lacoast.gov/new/Projects/Info.aspx?num=ba-39). For the purpose of this paper, the river channel study site is referred to as 'Bayou Dupont'. The channel bar is located between river kilometer (RK) 101 and RK 105, measured as distance upstream from the mouth of the LMR at the Head of Passes. The channel bar is predominately composed of sands approximately 0·13 to 0·25 mm in diameter. The first bathymetric survey conducted after the cessation of the dredging activity (i.e. the first post-dredge survey) occurred in May 2010; at that time the borrow pit was 280 000 m^2 in area and 1·46 million m^3 in volume. Dredge operators reported that significant borrow-pit infilling occurred during the dredging period (Moffatt and Nichol, 2012b) so it is likely that the borrow pit experienced significant evolution between the actual cessation of dredging and when the first post-dredge survey was completed. The maximum dredge depth likely never exceeded an elevation of −21·3 m NAVD88 (i.e. the North American Vertical Datum of 1988); the lowest permitted dredge elevation for that project.

In August 2012, a ~0·1 km^2 fraction of the Bayou Dupont borrow area was re-dredged by the US Army Corps of Engineers (USACE) to provide material for a salt water sill located at the downstream end of the channel bar. The sill was a temporary submarine berm (8 m high, on average) constructed laterally across the channel thalweg to block the intrusion of salt sea water progressing up the Mississippi River channel (Fagerburg and Alexander, 1994). This salt water intrusion typically initiates during low river discharges (<5660 $m^3 s^{-1}$) and may threaten the water supply of the New Orleans, Louisiana and other communities at discharges lower than 2900 $m^3 s^{-1}$.

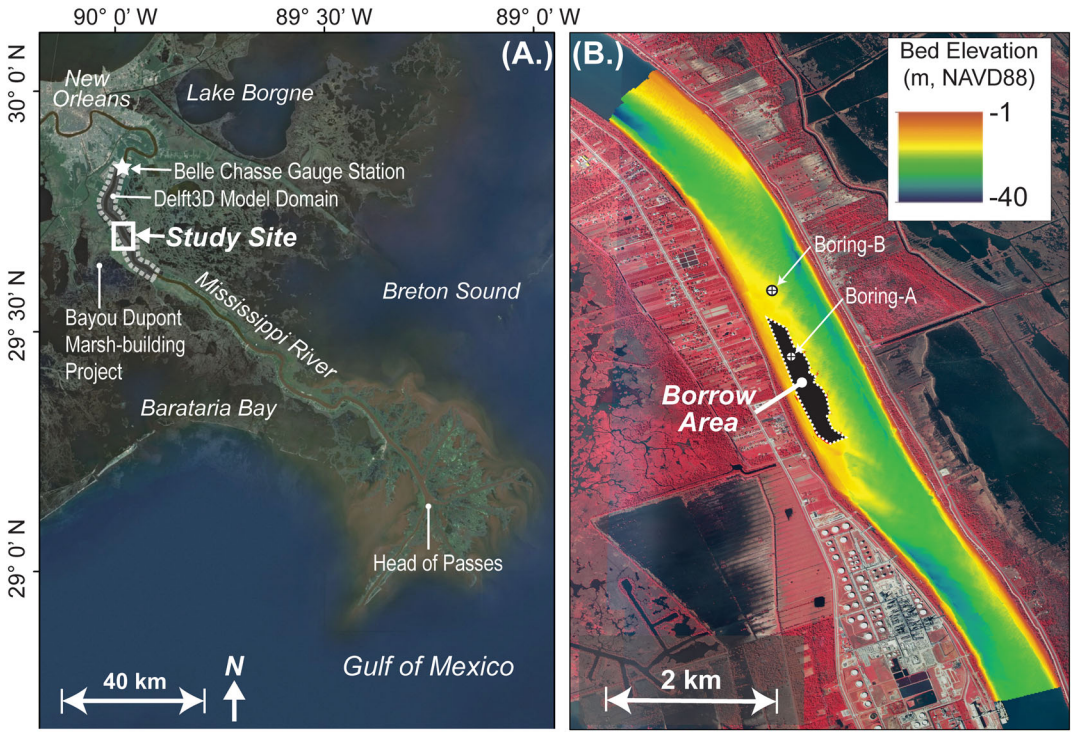

Figure 1. Regional (A) and reach-scale (B) maps of the study area in the lower Mississippi River, Louisiana, USA. The black polygon in B, shows the approximate extent of borrow-pit area dredged in the lateral bar to at least a depth of 2·5 m prior to March 2010. The location of borings collected in April 2012 (discussed in the Results section) are also plotted. This figure is available in colour online at wileyonlinelibrary.com/journal/espl

Methods

The study methods consist of three main components. The first component is an investigation of a time series of bathymetric surveys that document the morphological evolution of a LMR channel bar borrow pit. Rates of borrow-pit infilling were calculated from differencing the bathymetric surveys and accounting for the length of the inter-survey time period. The second component is the collection and analysis of observed river discharge and sediment transport data at the up-stream boundary of the study area to estimate flow and sediment dynamics within the borrow-pit area which has little observed data available. In the third component, a field data-calibrated numerical model was employed to estimate the river hydrodynamics around idealized and observed borrow-pit geometries and to explore the temporal and spatial relationships between local metrics of flow, in terms of boundary shear stress or 'bed stress', and the observations of infilling. The model was also employed to execute a scenario that estimated the amount of sand transport routed into the borrow pit by river flow.

Calculation of borrow-pit infilling

Bathymetric survey data were collected over a 2·5 year time period at the study site using both single beam and multibeam sonar imaging. A total of seven surveys were conducted, beginning with one pre-dredge survey on August 2009 and continuing at irregular intervals after the dredging was completed in May 2010, January 2011, April 2011, May 2011, August 2011, and October 2012. The survey timing was based on the priorities of state and federal management agencies charged with monitoring the borrow area. The survey data were interpolated to raster digital-elevation models (DEMs) using the ESRI ArcGIS (http://www.esri.com/) environment. The horizontal resolution (cell size) of the DEMs were dependent on the resolution of the processed sonar datasets archived by the State of Louisiana/USACE and ranged from 1 to 8·5 m^2. Further description of the bathymetric survey methods is included in the online Supporting Information.

Infilling rates were computed by first differencing the elevation (i.e. DEM raster cell values) of each consecutive survey and then by dividing the results by the length of the time intervals between the surveys. To quantify regional patterns of infilling (or erosion) occurring within different areas of the borrow pit and the proximal channel bar, spatially-averaged infilling rates for 11 sub-regions of the study site were computed (Figure 2). Eight of the sub-regions compose the borrow pit (P1–P8). There are three additional sub-regions located immediately upstream (Up), downstream (Down), and laterally adjacent (East) relative to the borrow-pit location. To further identify infilling trends through the study site, elevation was measured along a longitudinal transect, *X*–*X*′. This transect is also used to explore the results of the modeling experiments discussed later in this section.

Visual analysis of the October 2012 survey DEM indicated that a fraction of the study site, including approximately 25% of the upstream half of the borrow pit, was impacted by the USACE sill dredging that occurred in August 2012. To mitigate the effects of the sill dredging on the infilling calculations, the sill borrow-pit area was clipped from the October 2012 DEM and replaced with elevation values predicted by linearly extrapolating the surrounding topography through the clipped area. This procedure reduces the precision of the elevation data in the clipped area but should preserve broader spatial trends.

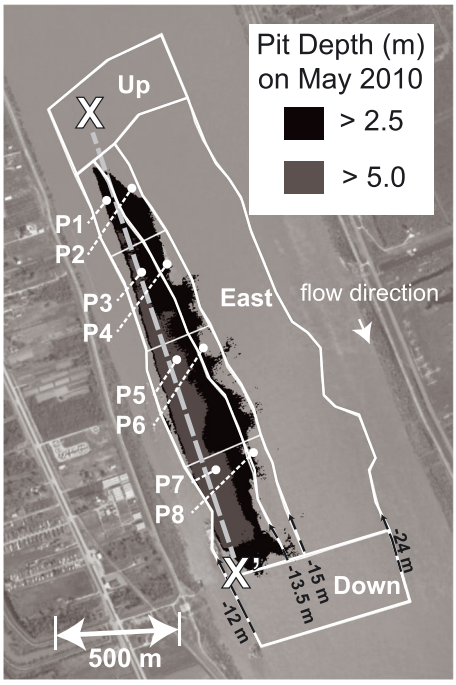

Figure 2. Map of the eight borrow-pit sub-regions (P1–P8) and three proximal bar sub-regions (Up, Down, East) for which sediment infilling was analyzed. The black/dark gray areas on the channel bed shows the approximate location of the main borrow pit. The longitudinal boundaries of these sub-regions are aligned with the pre-dredged elevation contours, −12, −13·5, −15, and −24 m NAVD88. This map also shows the location of transect X–X′ used for additional analyses in this study.

Estimation of flow and sand transport at the up-stream boundary of the study area

The flow at the Bayou Dupont study site was estimated based on river discharge data collected at or near the US Geological Survey (USGS) river gauge station located at Belle Chasse, Louisiana (USGS gauge number 07374525). High river discharges are truncated downstream of New Orleans due to the operation of the Bonnet Carré spillway (located at RK 206) which is designed to divert up to 7100 $m^3 s^{-1}$ of river water into Lake Pontchartrain for flood control purposes. The USACE initiates spillway operation when the river stage exceeds 5·2 m NAVD88 at New Orleans which has occurred 10 times since 1937. The Belle Chasse station is the closest flow gauge to the study site (within 18 km) that collects near-instantaneous (six minute intervals) water measurements. River flow is measured at this station using a fixed, horizontal acoustic Doppler current profiler that was installed in 2008.

In addition to the river discharge data, fluvial sediment transport was estimated for the river reach proximal to the Belle Chasse station to provide upstream boundary condition data for the numerical modeling employed by this study. The fluvial transport of sand (sediment between 0·063 and 2·0 mm in diameter) was estimated by coupling a bedform transport (Q_B) rating curve with suspended sand (Q_{SS}) data reported in Allison *et al.* (2012):

$$Q_B = 146.3 \exp^{1.77E-4 \times Q} \quad (1)$$

$$Q_{SS} = 2.5 \times 10^{-4} Q^2 + 0.15Q - 3.3 \times 10^4 \quad (2)$$

where Q_B and Q_{SS} are in tonnes per day (T d^{-1}) and Q is river discharge in cubic meters per second ($m^3 s^{-1}$). Both functions

were derived using the Belle Chasse station flow data and sediment measurements collected in the proximal channel reach over the period of 2008 to 2010. Bedform transport was calculated using the bathymetric differencing technique outlined in Nittrouer *et al*. (2008). The suspended sand discharge was estimated from boat-based sediment concentration measurements recorded using a depth-integrated water sampling methodology (i.e. employing a D90-series isokinetic sampler at five standardized depths per measurement station) along a channel cross-section at three to seven stations. The sediment concentration values were multiplied by river discharge derived by boat-based acoustic Doppler current profiler (ADCP) measurements to calculate values of sediment flux. Equation (2) was derived for suspended sand transport by removing sediment smaller than 0·064 mm in diameter from the concentration measurements; sediment grains larger than sand (>2 mm in diameter) do not make up a significant fraction of the bed material in the LMR and were not observed in suspension during the study period). Five large lateral channel bars lie between the Belle Chasse channel reach and the study site that may impact sand transport between the two areas by serving as additional sediment sources or sinks depending on local flow conditions and sediment loads.

Further information on flow data collection using ADCP measurements at the Belle Chasse river gauge station and as deployed by boat is included in the online Supporting Information.

Numerical modeling

Numerical modeling scope

This study uses numerical modeling to simulate river hydrodynamics in and around 'idealized' and 'observed' borrow-pit geometries located on the Bayou Dupont channel bar. Model runs employing idealized pit geometries were to identify characteristic relationships between metrics of pit geometry (e.g. mean pit depth, total pit length) and bed stress (e.g. magnitude and spatial distribution). Model runs employing the observed borrow-pit geometries were to estimate the magnitudes and spatial distributions of bed stress within the observed borrow pit at specific time steps (i.e. the bathymetric survey dates).

Model overview

Flow and sediment transport were simulated using Delft3D, an open-source multidimensional river hydrodynamics and sediment modeling package. Delft3D computes flow by solving the Navier–Stokes equations of fluid motion and the equations of sediment transport and continuity on either a two- or three-dimensional curvilinear finite-difference grid. The model also offers a number of turbulence models for the modeler to choose from. The Delft3D code is well documented (http://oss.deltares.nl/web/delft3d) and it is routinely used by the research community to model river morphodynamics (e.g. Hajek and Edmonds, 2014; Matsubara and Howard, 2014; van Dijk *et al*., 2014). The model employed by this study is a modified version of that described in Gaweesh and Meselhe (in press).

An objective of the numerical modeling experiments in our study was to calculate the magnitude and spatial distribution of bed stress, the driver of sediment transport, in and around the borrow-pit area. Delft3D computes bed stress (τ_b), dependent on the two- or three-dimensional velocity profile, as:

$$\tau_b = \frac{\rho g U|U|}{C^2} \tag{3}$$

where ρ is the density of water, g is acceleration due to gravity, U is flow velocity and C is the Chezy roughness coefficient. For two-dimensional simulations, U is set as the magnitude of the depth-averaged horizontal velocity. For three-dimensional simulations, U is set as the horizontal velocity for first hydrodynamic layer of the model domain just above the river bed.

To simulate the three-dimensional river hydrodynamics in the study area, a computation grid was created to represent the LMR reach extending from RK 89·6 to RK 121·6. The grid cell width was approximately 5 m; grid cell length varied between 5 and 30 m, increasing with distance away from the borrow area. The vertical grid structure was composed of 30 vertical layers, stratified parabolically. The total grid height was dependent on the modeled river stage. The modeled bathymetry for the channel outside of the immediate study site was based on interpolation of the USACE decadal single-beam bathymetric survey; the bathymetry for the study site was derived from the bathymetric surveys discussed in the previous section.

Model scenarios

The hydrodynamic modeling scenarios (Table I) were developed to estimate parameters of the hydrodynamic flow field, specifically the flow velocity and bed stress, around and within the borrow-pit area. These scenarios employ four 'idealized' and four 'observed' borrow-pit geometries. The idealized geometries represent a rectangular borrow-pit morphology (250 m by 1600 m in area) dredged to one of four different uniform bed elevations (i.e. −15, −18, −20, and −22 m NAVD88).The observed pit geometries were extracted from the pre-dredge (i.e. August 2009), May 2010, January 2011, and the August 2011 bathymetric surveys. For each pit geometry, four different steady river discharges were simulated. To model a steady three-dimensional flow, Delft3D was run using a single discharge until an approximate steady-state condition was achieved. The four different discharge values were selected to simulate the typical range of flows in the

Table I. Summary of model scenarios simulated for this study

Scenario type	Bathymetry	Discharge(s)
Hydrodynamic: idealized geometries (uniform pit depths)	• pit bed elevation = −15 m • pit bed elevation = −18 m • pit bed elevation = −20 m • pit bed elevation = −22 m	• Low, 11 327 $m^3 s^{-1}$ • Moderate, 19 822 $m^3 s^{-1}$
Hydrodynamic: observed geometries (from survey data)	• observed pre-dredged bathy • borrow area = May 2010 • borrow area = January 2011 • borrow area = August 2011	• High, 28 317 $m^3 s^{-1}$ • Flood, 33 980 $m^3 s^{-1}$
Sediment transport	• borrow area = May 2010	• Observed hydrograph (May 2010–October 2012)

LMR: low (11 327 $m^3 s^{-1}$), moderate (19 822 $m^3 s^{-1}$), high (28 317 $m^3 s^{-1}$), and flood level (33 980 $m^3 s^{-1}$).

An additional scenario was setup to calculate the sand load that entered the borrow-pit area and that was available to contribute to the borrow-pit infilling during the study period. This scenario predicted non-cohesive sand transport using the van Rijn 1984 transport function which was partially developed using Mississippi River based data (Van Rijn, 1984a, 1984b). Sediment transport rates were prescribed at the upstream boundary of the model domain based on the sediment measurements collected within the Belle Chasse river reach. Very fine, fine and medium sand (i.e. median diameter equal to 0·083, 0·167, and 0·333 mm, respectively) were used to represent the sand classes dominant in the river (Allison *et al.*, 2012; Meselhe *et al.*, 2012; Ramirez and Allison, 2013). The estimated spatial variation of the sediment thickness and bed stratification was mapped into the model to differentiate between sediment-rich areas (e.g. alternating sandbars) and areas where no dune migration was assumed (e.g. thalweg line and deep holes at river bends) (Allison and Nittrouer 2004). The sediment thickness linearly varied between 10 m and zero, while bedrock was assumed to exist at an elevation of −35 m NAVD88. This scenario employed the model domain and bathymetry used in the May 2010 hydrodynamic scenarios but with the horizontal resolution reduced by a factor of two and simulated in two-dimensions for computational efficiency. The objective of this scenario was to predict the volumetric flux of sandy sediment into the Bayou Dupont borrow area rather than to simulate the morphological evolution of the borrow pit, therefore, the mobile bed capabilities of Delft3D were not employed. This modeling technique was necessary because of the relative absence of observational sediment transport measurements available at or nearby the borrow area.

Model calibration

Model hydrodynamics were calibrated against observed depth-averaged flow velocities and vertical-velocity profiles. Bed roughness was used as a key variable during calibration tests. Initial calibration was completed using observed flow velocities acquired at five cross-sectional river transects distributed throughout the model domain using boat-based ADCP velocity measurements during a 19 822 $m^3 s^{-1}$ river discharge (April 7, 2009 survey date). Generally, model performance was in good agreement with the measurements, with an average coefficient of determination value (r^2) of approximately 0·82 (Legates and McCabe, 1999), an average bias of 5·3%, and an average mean error of 0·18 $m s^{-1}$ (Meselhe and Rodrique, 2013). An additional test was executed to confirm model performance using observed flow data derived from 14 ADCP transects at a 23 251 $m^3 s^{-1}$ river discharge (April 13, 2010 survey date). Performance metrics from this test had an average r^2 of 0·85, a percent bias of 2·7%, and a mean average error of 0·22 $m s^{-1}$. Calibration tests found that a Chezy roughness value of 65 reproduced the most realistic hydrodynamic environment; this value is approximate to Manning's roughness coefficients (0·024 to 0·026 dependent on flow depth) that are routinely used to estimate flow velocity in the Mississippi River (e.g. Jordan, 1965). The key model parameters selected for use in this study following model calibration are shown in Table II.

Table II. Key model calibration parameters used in each model scenario

Scenario type	Model parameter	Value(s)
Hydrodynamic	computational time step	0·1 min
	Three-dimensional turbulence closure method	k-Epsilon
	computational time step	0·3 min
Sediment Transport	bedload function	Van Rijn, 1984a, 1984b
	Van Rijn reference height	1·5 m
	active layer thickness	0·5 m
	suspended sediment transport	advection-diffusion
Both	bed roughness	Chezy = 65
	horizontal eddy viscosity	0·1 $m^2 s^{-1}$

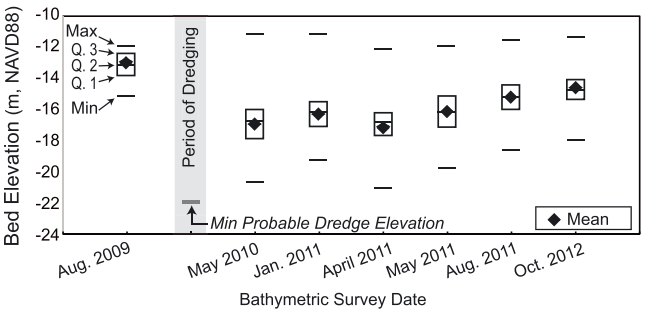

Figure 3. Summary statistics of the bed elevation values computed for the borrow-pit area from each of the seven bathymetric datasets. The first, second, and third quartile values are abbreviated as Q.1, Q.2, and Q.3, respectively.

Results

Field observations of borrow-pit infilling

Figure 3 shows the observed bed elevations for the borrow-pit area calculated from the bathymetric DEMs analyzed in this study. The borrow-pit area was differentiated as the bar area located within the eight borrow-pit sub-regions shown in Figure 2. The initial, pre-dredge elevation of the borrow-pit area ranged from −12 to −15 m (NAVD88), averaging −13·14 m. Dredging likely decreased the borrow-pit elevation by up to 9 m, to values approaching −22 m which is the minimum dredge-elevation permitted by law at this site. The mean borrow-pit elevation was −16·7 m during the first post-dredge bathymetric survey (May 2010) and increased to −14·73 during the last post-dredge survey (October 2012). Between May 2010 and October 2012, the mean borrow-pit elevation increased at an average rate of 0·88 m per year. The borrow pit increased in elevation during each inter-survey time period except between January 2011 and April 2011.

Figure 4 shows the longitudinal transect *X*–*X*′ of the channel bar bathymetry for multiple survey time periods. The August 2011 data indicate that some locations (i.e. the upstream third)

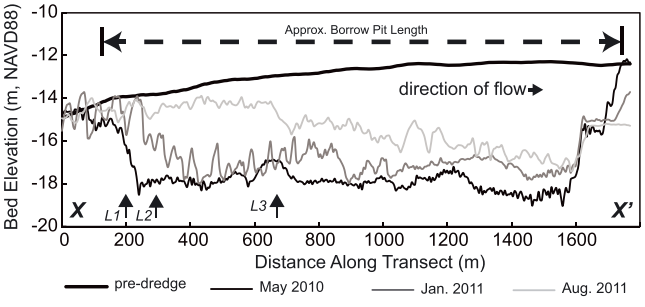

Figure 4. Bed elevation transect X–X′ computed from the bathymetric datasets. The location of the transect is shown in Figure 2. Arrows labeled L1, L2, and L3 show the approximated location of the upstream edge of the borrow in May 2010, January 2011, and August 2011, respectively.

of the borrow pit were approaching the pre-dredged elevation while other areas experienced much less change. Figure 4 also shows that a large fraction of the longitudinal variation in elevation occurred at length scales less than 100 m. Much of this variation was due to the presence of large mobile bedforms that had typical heights approaching 0·5 m and wavelengths near 20 m within the pit.

Table III summarizes the calculated sediment infilling that occurred in the study site during each inter-survey period. Table III includes the spatially-averaged values for each sub-region as well as the average value for the borrow pit and the outer channel bar areas. The extents of the bathymetric surveys were not uniform so data coverage in each of the outer sub-regions (i.e. Up, Down, East) varied between surveys. Analysis of two geotechnical borings collected within the study site (the boring locations are shown in Figure 1) in April 2012 indicate that the newly deposited material was similar in texture as the initial bar material (see online Supporting Information for a full description of this analysis).

A comparison of the infilling rates in the borrow-pit sub-regions indicates that the maximum amount of infilling initially occurred at the upstream-edge of the borrow-pit area and translated downstream over time. There was also a tendency for the deeper sub-regions in the eastern half of the pit to infill at greater rates than the shallower western sub-regions when the average bed depths were standardized by initial depth (i.e. accounting for the fact that initially deeper pit regions can accommodate more total infilling than shallower regions). Over the study interval, the spatially and temporally averaged infilling rates for the borrow-pit sub-regions P1 and P2 (i.e. the upstream most sub-regions), P3 and P4, P5 and P6, and P7 and P8 (i.e. the downstream most sub-regions) were 0·46, 0·40, 0·37, and 0·13 m yr^{-1} per meter pit-depth respectively. The average infilling rates for the eastern (P2, P4, P6, and P8) and western (P1, P3, P5, and P7) sub-regions were 0·43 and 0·26 m yr^{-1} per meter pit-depth respectively. Figure 5 shows the spatial distribution and degree of infilling computed for each inter-survey period.

The average rates of pit infilling tended to scale temporally with the elevation changes observed in the outer bar area, indicating that the infilling rate likely had some dependence on the bar-wide sediment dynamics. For example, between January 2011 and April 2011, both the borrow-pit area and the outer channel bar experienced relatively large values of net erosion. This could indicate that, during this time period, the channel bar was experiencing general deflation which temporarily overwhelmed any infilling processes active within the borrow pit. Further, Figure 5 shows that many areas of the borrow pit that experienced infilling correspond to the location of large bedforms which are the product of the bar-wide sediment dynamics rather than infilling processes. In the elevation-change maps (Figure 5), the locations of these bedforms appear as large curved stripes organized perpendicular to the flow direction. The three outer bar sub-regions experienced a loss of mean bed elevation during the first inter-survey period that included the initial dredging (August 2009 to May 2010). It is unclear if the magnitude of this apparent erosion outside of the borrow pit was influenced by the dredging operation, directly, from errant dredging, or indirectly, from the effects of the reduction to the local sediment supply.

Estimated flow and sand transport near the Belle Chasse river gauge station

The range of flows and sand transport rates computed for the LMR at the Belle Chasse river gauge station (i.e. at the upstream boundary of the study area) is shown in Figure 6. During the dredging period, the river experienced multiple hydrograph peaks, fluctuating between 15 000 and 30 000 $m^3 s^{-1}$. The Mississippi River experienced a record flood in 2011, exceeding 37 000 $m^3 s^{-1}$. During the peak of the flood hydrograph (May 9 through June 20), the USACE opened the Bonnet Carré spillway, located 101 km upstream of the Bayou Dupont channel bar, as a flood control measure, which limited river flow through the study area. The timing of the rising limb of the 2011 flood hydrograph corresponds to the inter-survey period when the borrow-pit bed experienced net erosion (i.e. January to April 2011). In 2012, the river experienced a spring peak near 29 700 $m^3 s^{-1}$ followed by a period of very low flow (~ 5000 $m^3 s^{-1}$).

Table III. Spatially averaged infilling for each inter-survey time period for each sub-region identified in Figure 2

	Infilling between surveys (m)											
Sub-region	August 2009–May 2010		May 2010–January 2011		January 2011–April 2011		April 2011–May 2011		May 2011–August 2011		August 2011–October 2012	
					Borrow pit							
P1	–2·57		0·67	(26·1)	–0·55	(4·5)	0·87	(38·5)	0·74	(67·2)	0·04	(68·9)
P2	–2·53		1·33	(52·6)	–0·26	(42·2)	0·57	(64·8)	0·39	(80·1)	0·13	(85·4)
P3	–4·02		0·67	(16·8)	–0·74	(–1·6)	0·76	(17·2)	1·60	(57·1)	0·29	(64·3)
P4	–2·64		0·72	(27·1)	–0·51	(7·9)	1·44	(62·4)	0·01	(63·0)	0·57	(84·7)
P5	–4·56		0·61	(13·3)	–0·72	(–2·5)	0·78	(14·5)	1·07	(38·1)	0·64	(52·2)
P6	–2·50		0·42	(16·7)	–0·81	(–15·6)	1·03	(25·4)	0·98	(64·5)	0·49	(84·1)
P7	–4·27		0·57	(13·4)	–0·97	(–9·2)	0·39	(0·0)	0·79	(18·5)	0·48	(29·7)
P8	–1·94		0·12	(6·4)	–1·01	(–45·6)	0·35	(–27·7)	0·83	(15·1)	0·65	(48·3)
Average	–3·55		0·63		–0·74		0·72		0·88		0·45	
Average rate per year			0·89		–4·22		6·12		3·38		0·38	
					Outer bar							
Up	–0·41		0·00		–0·70		0·24		0·64		0·10	
East	–1·39		0·41		–0·36		–0·14		0·43		–0·17	
Down	–1·65		0·11		–1·10		–0·22		0·58		1·80	
Average	–1·36		0·26		–0·64		–0·12		0·47		0·27	

Note: Values in parentheses represent the cumulative percentage of the initial borrow-pit depth that has infilled by the conclusion of that period.

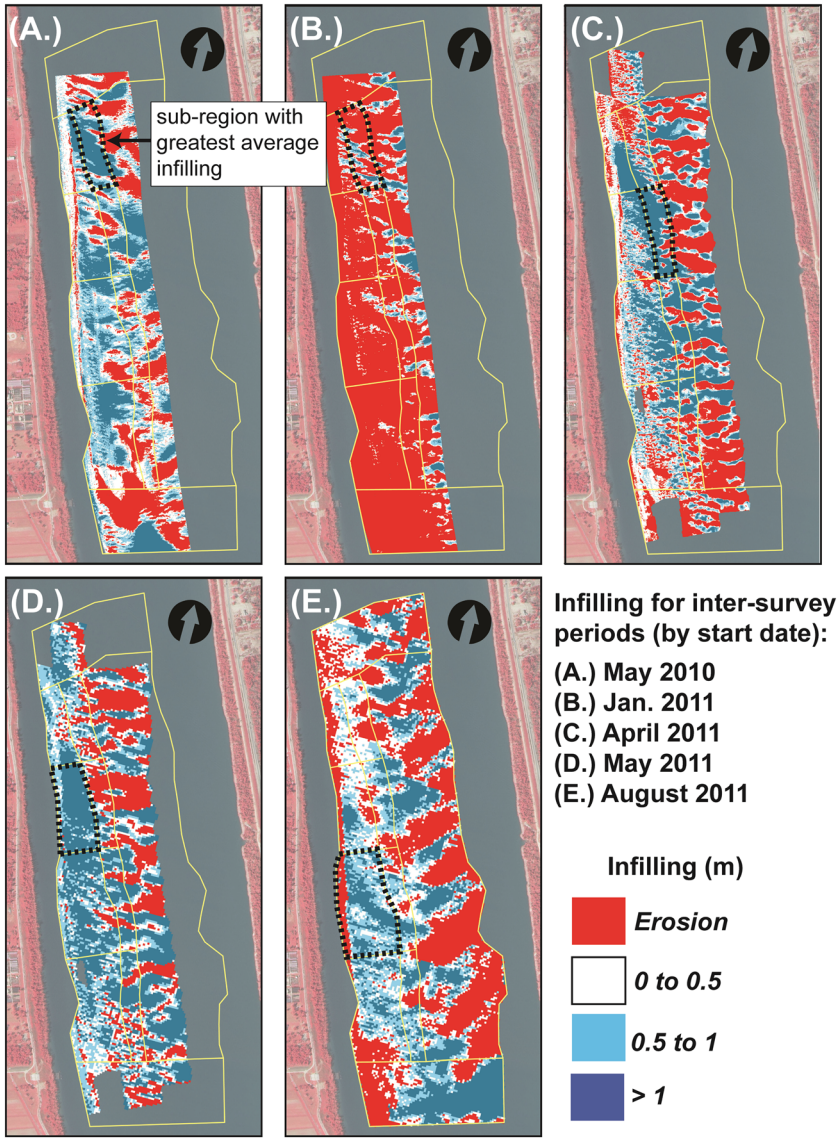

Figure 5. Maps showing the infilling computed for five inter-survey time periods. The black dashed polygon identifies the sub-region that experienced the greatest average infilling for each inter-survey period. This figure is available in colour online at wileyonlinelibrary.com/journal/espl

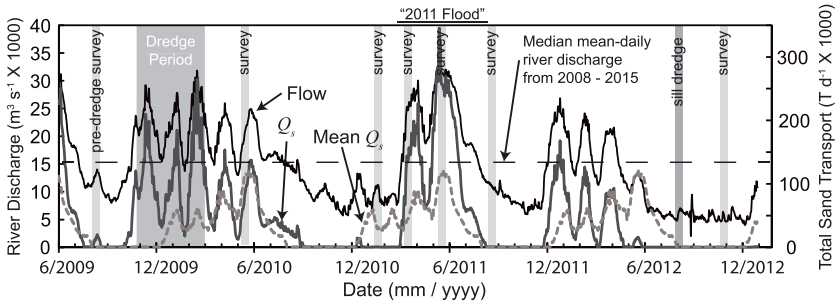

Figure 6. Flow discharge and combined suspended and bedload sand transport (Q_s) calculated for the lower Mississippi River near Belle Chasse, Louisiana (location shown in Figure 1) for the study period. The plot shows the relative timing of the dredging, bathymetric surveys, and 2011 river flood. The black dashed line shows the median mean-daily river discharge for the period of gauge operation, 2008–2015. The gray dashed line shows the estimated mean-daily sand flux calculated using the average-annual hydrograph and Equations (1) and (2). This figure is available in colour online at wileyonlinelibrary.com/journal/espl

Typically in the LMR, rates of total sand transport do not become significant until river discharge exceeds 10 000 $m^3 s^{-1}$, which is the approximate threshold at which sand becomes suspended in flow (Ramirez and Allison, 2013). The discharge record over the study interval indicates that little sand was in transport (1) between August 2010 and April 2011, (2) between August 2011 and December 2011, and (3) from May 2012 through to the end of the study (i.e. October 2012).

Results of the hydrodynamic numerical model scenarios

The hydrodynamic model scenarios that employed idealized borrow-pit geometries predicted that the borrow pit significantly impacted the hydraulics of the full depth profile of the flow. Figure 7 illustrates how the model predicted that the borrow

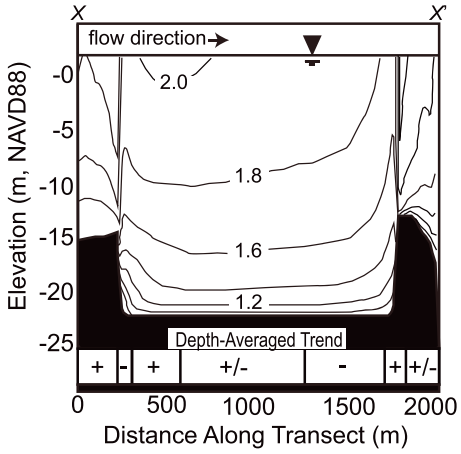

Figure 7. Modeled flow velocity (in m s^{-1}) profile along a central longitudinal transect X–X′ of the borrow-pit area. The data are derived from the model scenario employing the borrow pit with the idealized bed elevation at −22 m NAVD88 and the 'high' river discharge. The depth-averaged trend, in terms of flow acceleration (+) and deceleration (−) is shown at the bottom of the plot.

pit typically reduced flow velocities relative to the upstream values in two distinct areas along the transect X–X′, (1) as flow initially enters the borrow pit and (2) as the flow approaches the downstream edge of the borrow pit. As a flow volume entered the borrow pit, the flow velocity was reduced by up to 20% of the value computed immediately upstream and remained generally below the pre-dredged values along the entire length of the borrow pit. Figure 8 shows how bed stress varied along the same longitudinal transect for four borrow-pit geometries and two river discharges. Within the borrow pit, values of bed stress were lowest at the immediate upstream edge of the pit and increased at a decreasing rate with distance downstream, approaching the pre-dredged value after approximately 1000 m. Bed stress was also relatively low at the very downstream edge of the borrow pit as the flow velocity slowed upon approaching the pit wall. The model predicted that bed stress abruptly increased immediately downstream of the pit as the flow accelerated to accommodate the reduction in flow depth. In general, the model results predicted that the magnitude of bed stress within the borrow pit was strongly dependent on the borrow-pit depth and longitudinal position within the pit. While the absolute magnitude of the spatial variation in bed stress was also dependent on the river discharge, bed stress expressed as a percentage of the pre-dredged value only varied by $\pm < 0{\cdot}5\%$ due to changes in the discharge value.

Results of the sediment transport model scenario

The volume of sand predicted to enter the study site over the 2·5 year study period was estimated by the Delft3D sediment transport scenario and is summarized in Figure 9. Using the sand transport values calculated from measurements at or near the Belle Chasse river gauge station to populate the upstream sediment boundary conditions, the model predicted approximately 68 million tonnes (T) of sandy sediment entered the study site river reach; of that volume, 40% was predicted to have been routed to the borrow-pit area (which spans 20 to 30% of the total wetted width of the channel). Approximately 95% of the sediment routed into the borrow-pit area entered through the upstream edge. Within the study site, 3 to 4% of the predicted longitudinal (parallel to the mean flow direction) sediment transport was bedload and 10 to 15% of the predicted lateral transport was bedload. The model did not update bed bathymetry in response to sediment deposition or erosion so the results of this scenario cannot be used to directly calculate a reach-scale sediment budget.

Discussion

Observed patterns of infilling

The bathymetric datasets do not record a coherent temporal pattern of borrow-pit infilling. Despite the dense time series of observations reported in this study relative to other similar datasets (e.g. Rempel and Church, 2009; Owen *et al.*, 2012), the length of the time series was not long enough to define a statistically significant trend given the high variability of the mean inter-survey infilling rates, which range from $-4{\cdot}22$ m yr^{-1} (erosion) to $6{\cdot}12$ m yr^{-1}. Fitting a linear trend line to the field data and extrapolating the trend into the future predicted that the time required for the observed borrow pit to completely infill was 4·4 years.

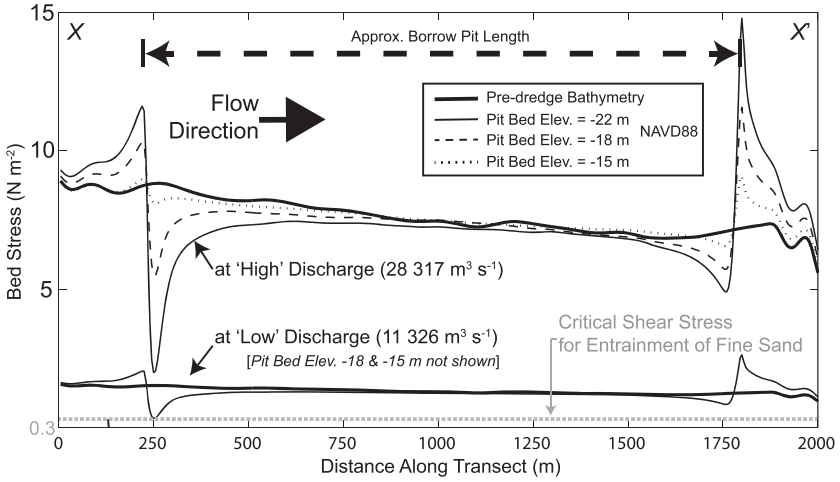

Figure 8. The predicted bed stress along transect X–X′ for multiple idealized pit geometries and the pre-dredged channel and two simulated discharges.

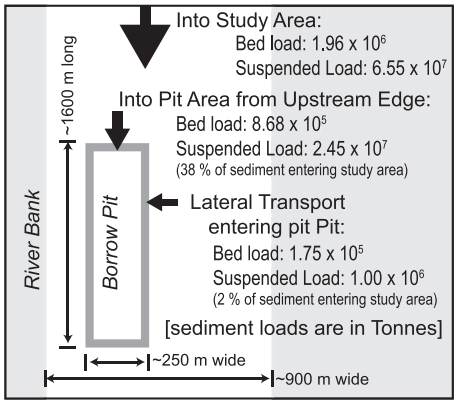

Figure 9. Predicted accumulated volume of sandy suspended and bedload transport entering the study area between May 2010 and October 2012. Percentage values show the fraction of the total sand input that enter the borrow pit during the study interval.

If the erosional period between January 2011 and April 2011 was removed as an anomalous data point from the dataset by only considering data from after that period (April 2011 to October 2012), the temporal pattern of infilling appeared logarithmic, with the rate steadily decelerating over time. In this case, when infilling was characterized as a logarithmic function rather than a linear trend line, the time required to infill the May 2010 borrow pit increased to 5·9 years. A previous modeling study of borrow-pit infilling in the LMR (i.e. Moffatt and Nichol, 2012b) found that infilling rates tended to follow a logarithmic rather than a linear pattern over time periods between one to three years. However, past research on the morphology of the LMR channel (e.g. Davies, 1966; Ray, 1979; Ramirez and Allison, 2013) indicates that alternating periods of bar- or reach-scale bed erosion and aggradation may be commonplace at sub-annual timescales, suggesting that a period of bar-wide erosion may not be anomalous within the study period. The period of channel bar erosion identified in this study (i.e. spring 2011) was characterized by rapid fluctuations in river discharge which may have temporarily decoupled the typical balance between the channel sediment transport capacity and the amount of sediment supplied by upstream sources (assumed to be channel bars not further than tens of kilometers upstream). The mean spring-time sand transport rate for the LMR at Belle Chasse relative to that estimated for 2011 is shown in Figure 6. The rapid rise of the 2011 Mississippi flood hydrograph suddenly increased the sand transport capacity by approximately 200% of the mean spring-time value.

Perhaps the most coherent spatial pattern identified in the observed infilling dataset was the downstream translation of the zone within the borrow pit that contained the highest local infilling rates. This zone was generally located immediately downstream of the upstream-edge of the borrow pit, which itself translated downstream over time (identifiable in Figures 4 and 5). The hypothesized processes causing this pattern include: (1) as flow passed over the steep elevation gradient located at the transition between the upstream channel and the borrow pit, the sediment transport capacity of the flow declined due to the sudden drop in bed stress; (2) in response to the reduced transport capacity, sediment drops from the flow and becomes deposited in the pit; (3) the rate of sediment deposition decreased with downstream distance due to a gradual decline in the bed stress gradient; (4) this differential in sediment deposition allowed upstream pit areas to infill and return to their pre-dredge elevation faster than downstream areas; (5) once an upstream area sufficiently infilled, its hydrodynamics (velocities and bed stresses) returned to its pre-dredged state and the channel-pit transition zone shifted to a position downstream of that area. This pattern is suggestive of results reported in previous modeling studies (e.g. Fredsoe, 1979; Ponce *et al.*, 1979; van Rijn, 1986) which also typically identified a tendency for the channel bed immediately downstream of the borrow pit to erode as flow was accelerated out of the relatively deep pit into the shallower channel. The modeling studies predicted that, coupled with the selective infilling occurring at the upstream zone of the borrow pit, the erosion of the downstream channel bed would cause the apparent position of the borrow pit to translate in the downstream direction. While some bed erosion was observed downstream of the Bayou Dupont borrow pit, the observed pit position remained relatively stable during the period of analysis.

Similar to borrow-pit infilling, infilling rates in surface-water reservoirs located upstream of river dams are typically greatest at the transition between the incoming river channel and the reservoir basin (Morris and Fan, 1997). However, the bed stress gradient is much steeper in reservoirs than river-channel borrow pits as the flow velocity is reduced to near zero in the reservoir pool, as opposed to within the observed borrow pit, where the flow velocity was only reduced by a maximum of 20% of value immediately upstream. Because of this difference, models of reservoir infilling, which are often based on the mechanics of delta propagation (Morris *et al.*, 2008), are not likely applicable to borrow-pit infilling.

The effects of borrow-pit geometry on predicted bed stress

To identify how metrics of borrow-pit geometry affected the local bed-stress field, predicted values of bed stress for the initial pre-dredged channel bathymetry and the idealized borrow-pit geometries were computed along the transect X–X′ and averaged at 200 m intervals. The ratio of the pre-dredged and borrow-pit bed stress values, referred to herein as the bed-stress reduction ratio (R^*),

$$R^* = \tau_b/\tau_{b0} \tag{4}$$

where τ_{b0} is the initial pre-dredge bed stress, were calculated for each pit geometry and simulated river discharge. However, as discussed in the hydrodynamic-modeling results section, the relative ratios of τ_{b0} *and* τ_b for each modeled pit geometry were relatively insensitive to flow discharge so it is assumed that the effect of discharge on R^* can be neglected from further analyses.

Comparison of R^* and metrics of pit geometry found that R^* decreased with borrow-pit depth below the initial pre-dredge channel elevation (d) and with horizontal distance from the upstream-edge of the borrow pit (x_p). Values of R^* scaled linearly with d and exhibited a more complex relationship with x_p. Values of R^* increased logarithmically with x_p except in a small area of the pit bed very near the downstream-edge of the pit. In this area, the downstream edge of the borrow pit obstructed the approaching flow and reduced the horizontal velocity of the flow to near zero (as observed in Figure 7). This reduction in flow velocity led to a localized decrease in R^* with increasing x_p until the flow volume was routed up and out of the pit into the channel downstream.

The dependence of R^* on d agrees with the mathematical analysis in van Rijn and Walstra (2002), which predicts that the difference between the upsteam flow velocity (U_o) and the velocity in the borrow pit (U_{PIT}) would scale with ratio of

the initial flow depth (h_o) and the flow depth in the borrow-pit area (h_{PIT}) in accordance with the continuity equation:

$$U_{PIT} = U_o(h_o/h_{PIT}). \quad (5)$$

The range of borrow-pit depths examined in this study typically increased overall flow depths by 10 to 30% of the pre-dredged value and resulted in the same approximate percentage decrease in depth-averaged flow velocities within the borrow pit. As suggested by Equation (3), the reduction in bed stress scaled with the square of reduced flow velocities.

Figure 10 summarizes the relationship between R^*, d, and x_p. Near the upstream-edge of the borrow pit, R^* values are below 0·9 for pit depths exceeding 3 m and below 0·8 for pit depths exceeding 6 m. For reference, the USACE may permit dredge depths down to 15 m below the channel bed level within the LMR dependent on local channel and flood-control levee properties (Moffatt and Nichol, 2012a).

The relationship between predicted bed stress and observations of borrow-pit infilling

To quantify how bed stress, in terms of the bed stress reduction ratio (R^*), affected borrow-pit infilling, R^* values for the observed borrow-pit geometries (i.e. May 2010, January 2011, and August 2011) were computed along the longitudinal transect X–X′ at 10 m intervals. These values were then compared to the magnitude of observed infilling that occurred during the following inter-survey period along the same longitudinal transect.

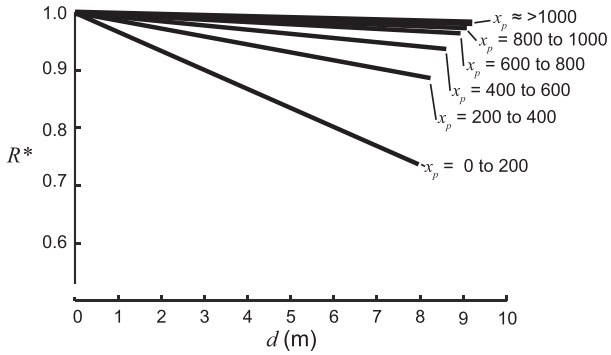

Figure 10. The modeled relationship between borrow-pit depth (d) and spatially-averaged R^* for 200 m longitudinal sections of a borrow pit with a total length of 1600 m. The relationships are fit by applying a linear trend line to the Delft3D model results.

Figure 11 shows the relationship between R^* and infilling within the borrow pit. Values of infilling were negatively correlated with R^*, using both standard (Pearson's) and non-parametric (Kendall's Tau) correlation tests. Non-parametric correlation was performed because the distribution of variable values did not meet the definition of a normal distribution at 95% confidence. Results shown in Figure 11 indicate that the further the bed stress deviated from its pre-dredged value (i.e. the pre-dredge R^* value = 1) at a given location, the more likely that location would experience bathymetric evolution during the following inter-survey period. Pit areas with bed stress significantly below the pre-dredged values were more likely to infill, while pit areas with bed stress above the pre-dredged value were more likely to erode. As areas with relatively low R^* values were typically associated with the deepest borrow-pit areas, the net result of this pattern of deposition and erosion would be gradual channel evolution back to its pre-dredge bathymetry.

An R^*-based modeling experiment to simulate borrow-pit infilling

To further examine the dependence of R^* on borrow-pit evolution, a reduced-complexity numerical-modeling experiment was devised. The objective of the modeling experiment was to test if the patterns of observed borrow-pit infilling could be accurately simulated using the simple relationships between borrow-pit geometry, bed stress, and pit bed evolution identified in this study. Reduced-complexity models have been increasingly used over the past decade to investigate the role of different geomorphic processes on landscape evolution by selectively activating or excluding specific aspects of the governing physics (Murray, 2007; Nicholas, 2010). The model computes sediment infilling longitudinally along a one-dimensional borrow pit based on R^* values estimated by locally-averaged pit depth and distance from the upstream edge of the borrow pit (i.e. d and x_p). A detailed description of the model of borrow-pit infilling used for this experiment is included in the online Supporting Information.

Results of the modeling experiment

The reduced-complexity modeling experiment calculated that over the 2·5 year study period, 55% of the initial borrow-pit

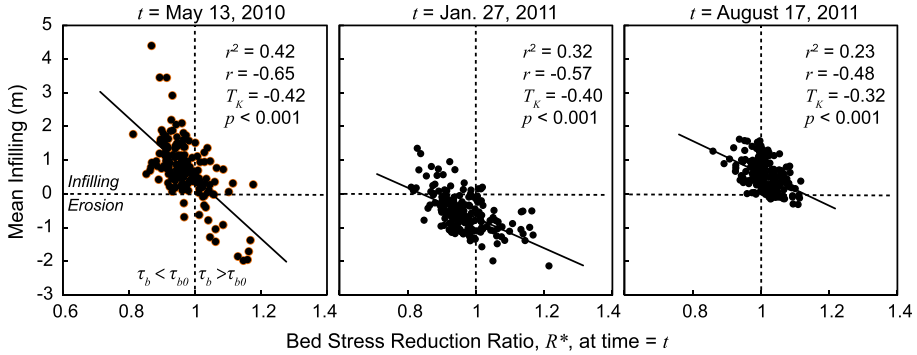

Figure 11. The relationship between modeled R^* and the observed sediment infilling for three survey periods (beginning May 2010, January 2011, and August 2011) along transect X–X′. The sediment infilling is calculated as the depth of the infilling observed during the following inter-survey period (e.g. for t = May 2010, the inter-survey period spans from that date to the next survey date, January 2011) averaged at 10 m intervals along the transect. In each plot the r^2 value is given for the linear regression trend line shown, as well as the Pearson's correlation coefficient (r) and Kendall's Tau coefficient (T_K). Each test coefficient is significant to at least 99·9% confidence.

volume (1·46 million m^3) would infill with sand. This calculated value is remarkably similar to the observed value derived from the bathymetric survey dataset (53%). Figure 12 shows both the calculated and the observed cumulative sediment infilling over the study period. The results of the modeling experiment generally resolve the temporal trend in the observed values, differentiating periods of relatively low and relatively high infilling; over each inter-survey period, the model typically predicted cumulative infilling within ± 5 to 50% of that observed. The modeling results did not reproduce the observed period of net erosion between January 2011 and April 2011. This may be because the modeling results estimated sediment supply as a simple function of upstream bed stress and cannot resolve hysteresis effects originating from sediment supply limitations. As discussed previously, the rise of the spring 2011 flood hydrograph rapidly increased the sediment transport capacity of the LMR. If upstream sediment supply was unable to keep pace with the increase in sediment transport capacity during this time period, sediment supply limited transport conditions would have prevailed or, if already present, become significantly enhanced.

The calculated pattern of the longitudinal borrow-pit infilling is illustrated in Figure 13. The model experiment predicted a slightly steeper longitudinal decline in cumulative infilling relative to that indicated by the final observed pit bathymetry. The model predicted that the initial upstream length of the borrow pit essentially infilled to the pre-dredge elevation while the elevation of the downstream margins of the borrow pit experienced little change or net erosion. The difference in the spatial pattern between the calculated and observed infilling is likely due to the simplicity of the employed model versus the complexity of the channel sediment dynamics. For example, the model predicts that sediment transport rates immediately adapt to the prescribed levels of bed stress, which is typically not the case in real-world fluvial environments (Phillips and Sutherland, 1989; Chen *et al.*, 2010; Gouverneur *et al.*, 2013), especially in turbulent, high-velocity flow, where sediment settling may experience significant lag effects (e.g. where horizontal velocity $>>$ sediment settling velocity) (Van Rijn and Walstra, 2002). A numerical modeling study by Knaapen and Kelly (2012) found that incorporating these lag

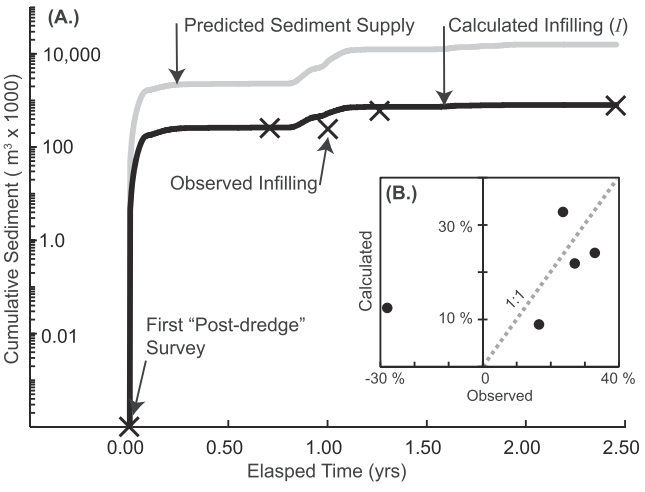

Figure 12. (A) Total sand transport into the borrow-pit area (sediment supply) and the fraction of that transport that was deposited within the pit (infilling) as calculated by the reduced-complexity model. Also shown are the observed values of infilling derived from the bathymetric surveys. Note that the datapoint for the April 2011 survey is negative and is not shown on this plot. Inset plot (B) shows the observed versus calculated percentages of the total infilling that occurred during each inter-survey period.

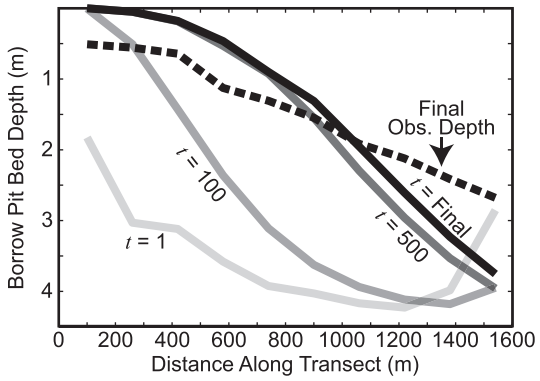

Figure 13. The calculated and observed (Obs.) borrow-pit bed bathymetry over the period of analysis. Infilling is computed at the centroid of each of the 10 longitudinal cells of the pit using spatially-averaged geometries and sediment transport values. Bed bathymetries are shown for four time intervals: 1, 100, 500, and 897 (Final) days.

effects in a physics-based trench infilling model reduced the longitudinal gradient of infilling and generally increased the predictive accuracy of the model. Further, a significant fraction of bed material transport in the LMR takes place through the translation of large bedforms (i.e. dunes). Recent research (Nittrouer *et al.*, 2008; Ramirez and Allison, 2013) has shown that these dunes may rapidly change size and position over short timescales (i.e. on the order of days) in response to the hydrodynamic environment. For example, Nittrouer *et al.* (2008) reports that dunes in the LMR routinely reach heights (3 m) that would approach the initial depth of the borrow pit during large river discharges ($> 20\,000\,m^3\,s^{-1}$), and that dune heights may even exceed 10 m during large floods. Bed material flux due to these large dunes creates unsteady modulations in the local sediment transport regime which may diffuse broader, more gradual temporal or spatial trends of bed evolution (McElroy and Mohrig, 2009) such as those caused by infilling processes.

The fact that the modeled values of cumulative borrow-pit infilling closely approximate the observed values suggest that the processes simulated within the model experiment may be adequate to predict borrow-pit infilling rates in Mississippi River channel bars and similar fluvial systems. The model calculates infilling as simple functions of only two types of parameters: sediment supply and borrow-pit geometry (i.e. borrow-pit depth and longitudinal length). The identification of the key parameters in this study offers insight into the key mechanics of infilling processes in general, improving our ability to build simple, accurate, and widely applicable tools to better manage sand mining in rivers. For example, models like that proposed earlier can be used to select a pit geometry that produces the fastest infilling rate. Figure 14 shows the results from three additional reduced-complexity modeling experiments that calculated cumulative infilling for a 1·5 million m^3 borrow pit with different initial bed depths (3, 5, 10 m). For each experiment, the mean-annual LMR hydrograph (calculated from the eight-year period of record at the Belle Chasse river gauge station) was cycled (one full cycle = one annual hydrograph) to predict sediment supply into the pit area until the borrow-pit depth became negligible (< 1 m). The initial conditions of the model domain were set so that an increase in the initial pit bed depth was offset by a decrease in the initial pit length to maintain a single initial pit volume (the initial pit footprint was rectangular with a uniform, flat bed and a constant 250 m pit width). Interpretation of the results of these idealized experiments indicate that relatively deeper borrow pits infill at significantly faster rates than elongated pits. Increasing the

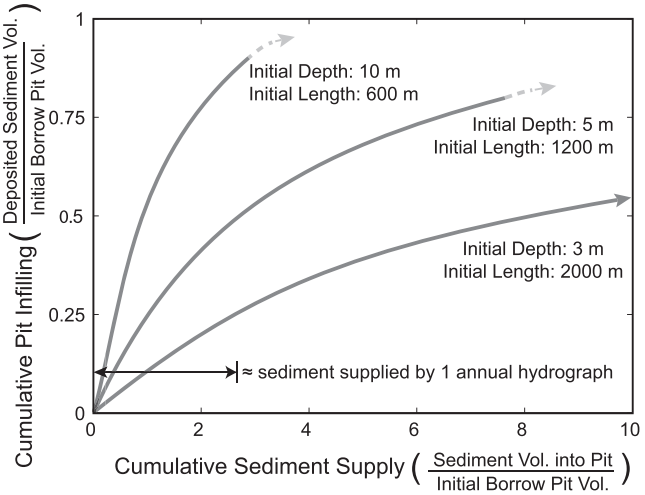

Figure 14. Modeled relationship between sediment supply, borrow-pit geometry (i.e. initial pit depth, and length), and borrow-pit infilling for a borrow pit with an initial volume of $1{\cdot}5 \times 10^6\ m^3$. Infilling for three different borrow-pit geometries are shown; initial pit volume and width are held constant. Both cumulative sediment supply and cumulative infilling are standardized by the initial borrow-pit volume.

initial borrow-pit depth from 3 m to 5 m, increased the mean infilling rate by a factor of three; increasing the initial pit depth from 3 m to 10 m, increased the mean infilling rate by a factor of eight. These results suggest that, to minimize the time required for a borrow-pit bed to infill to its approximate pre-dredged elevation, borrow-pit design should favor deeper rather than longer borrow-pit geometries. Reducing borrow-pit recovery time increases the frequency at which the borrow area can be sustainably mined (as defined in the Introduction) and reduces the duration in which the borrow pit would affect the natural flow and sediment transport regime of the river reach.

The impact of borrow pits on flow and sediment transport and its implications for channel recovery

This study helps to illustrate the direct impacts of a borrow pit on the local flow and sediment transport fields within the surrounding channel. From an engineering perspective, these impacts are significant because they influence the post-dredge evolution of the borrow pit, including the dimensions, location, lifespan of the pit, and the duration in which the pit will produce both direct and indirect reach-scale impacts on the channel morphology and sediment transport. If river engineers can accurately predict the extent and duration of these impacts, dredging operations can be better optimized to extract the maximum amount of borrow material while keeping the spatial and temporal extent of the affected environment to a minimum. The borrow pit analyzed in this study initially disrupted the local flow regime, reducing predicted flow velocities by up to 20%, but most of this disruption had likely dissipated within two to three years after dredging. Observations show that at the conclusion of the 2·5 year study period, over half of the borrow-pit volume had infilled with new sediment.

Interpretation of the results from the reduced-complexity modeling experiment indicate that the mean rate of infilling decreased as the borrow-pit depth decreased. As the borrow-pit depth returned to its pre-dredge elevation, the pit bed stress also returned to its pre-dredge value which increased the amount of sediment that was passed through the borrow-pit area rather than became deposited and stored within it. Modeled rates of infilling suggest that, within the first six months of the study period, 11% of the sand routed through the borrow-pit area was entrapped while, during the final six months of the study period, that value decreased to 5%. Model results also suggest that the borrow pit trapped less than 2% of the total sand entering the study site river reach over the study period, a result also supported from interpretation of the observed infilling data coupled with the Delft3D sediment transport predictions. Based on the modeling results and the observational data it is likely that sediment entrapment within the pit area, as well as the other reach-scale impacts, continued to decline with passing time. If the reduced-complexity model was run for an extended hypothetical time period that continually cycled the mean-annual LMR hydrograph, the model results estimate that a Bayou Dupont-size borrow pit would infill to more than 95% of its initial bed elevation 10 annual cycles after dredging. In this simplified case, the model results suggest that a 10 year interval between dredging campaigns may be necessary to ensure long-term sustainability of the borrow site. The ability of this type of model to accurately predict total infilling is uncertain as there are currently no validation observational datasets that document the full recovery of a borrow pit. In contrast to the reduced-complexity model results, the extrapolation of the observed infilling patterns (as identified at the beginning of the Discussion section) suggests that the pit may infill in less than six years.

Predictions of channel recovery relative to alternative field observations and geomorphic theory

Due to the relative scarcity of field studies on borrow-pit infilling in fluvial systems, there are few alternative observational datasets available to compare the results of this study. Rempel and Church (2009) examined the effects of in-stream mining on a gravel bar in the Fraser River, British Columbia, Canada, a river with bed sediment loads ($2{\cdot}5 \times 10^4\ T\ d^{-1}$) in the same order-of-magnitude as the Mississippi River. Approximately $1{\cdot}8 \times 10^5\ T$ of sediment was removed from the top of the bar by scalping, a mining technique that removes the top-most layer of sediment without excavating a true borrow pit, over a period of days. In three years, approximately 30% of the scalped sediment was replenished, with the vast majority of the new sediment deposited during one seasonal flood in the third year. Similarly, recent observations of channel bed evolution in response to moderate, repeated gravel mining in the Mad River, California, USA (typical sediment loads $\approx$ 60–800 T d^{-1}; mining removes $1{\cdot}12 \times 10^6\ T\ yr^{-1}$ of gravel, on average) suggest that sediment infilling at that location is primarily influenced by the peak river flows (Knuuti and McComas, 2003; Lehre *et al.*, 2009). Lehre *et al.* (2009) indicate that between 1993 and 2007, the mean annual rate of sediment infilling within the Mad River channel bed, as derived from topographic survey data, was correlated with the peak annual river discharge (which ranged from 433 to $1546\ m^3\ s^{-1}$ during the study period). Owen *et al.* (2012) reports observations of borrow-pit infilling within a small (bankfull discharge $\approx 500\ m^3\ s^{-1}$) sand-gravel river channel. The observed borrow pit (pit volume $\approx 400\ m^3$) was reported to have maintained a static position within the channel bed (no translation) and to have infilled in less than a year, primarily due to inputs of bedload sediment during a single flood event. The results of Rempel and Church (2009), Lehre *et al.* (2009), and Owen *et al.* (2012) suggest that, in beds with coarser

textured bed than the LMR, infilling processes may be much more pulsatory than that reported in this study, and are reliant on large flooding flows due to the lower relative mobility of the bed sediment.

Rovira *et al.* (2005a) performed a sediment budget of the lower Tordera River in Spain after a prolonged period of in-channel sediment mining. Approximately $8{\cdot}0 \times 10^6$ T of sand and gravel were removed from two large borrow pits within the channel bed over a 30 year period, lowering the reach-averaged bed elevation by 1·5 m. Over 15 years subsequent to the cessation of the mining, the affected channel reach infilled at rates approaching 12 mm yr^{-1}, suggesting that the channel bed would take at least 420 years to reach its pre-mining elevation. Considering the river reach receives approximately $1{\cdot}0 \times 10^5$ T of sediment influx annually (75% traveling as bedload) (Rovira *et al.*, 2005b), infilling processes would extract an estimated 18% of the sediment in active transport over that time period. This is a much higher sediment extraction rate than that reported in this study and may be more indicative of bedload dominated sediment transport regimes.

Channel evolution is the primary process that a river uses to optimize transport of its load of water and sediment (Lane, 1955; Kirkby, 1976; Huang and Nanson, 2000). Theoretically, optimal transport is accomplished by adjusting the channel network to evenly distribute and minimize energy dissipation (Langbein and Leopold, 1964; Yang, 1976). As discussed in this paper, dredging drastically disturbs the morphology and sediment transport capacity of the local river channel. This disrupts the equilibrium energy balance indicative of the undisturbed condition of the river in its steady-state (Simon, 1992). According to theory, a river will respond to this imbalance by shifting its hydraulic geometry and sediment load to increase energy dissipation at the site of the disruption. However, the rate at which the river can make these shifts is dependent on certain geomorphic properties of the fluvial system and the nature of the disturbance. The results of this study help identify which geomorphic properties are most influential in determining the rate of river response to disturbance, adding real world context to the general theories of river channel and landscape evolution (e.g. Chorley, 1962; Phillips, 2003).

For the Bayou Dupont study site, river response to mining-related disturbances is heavily influenced by local sediment supply and the borrow-pit geometry which is a first-order control of the bed stress within the pit. Mississippi River engineers and planners should focus monitoring efforts on these properties as they seek to identify sustainable mining practices. These properties may also play key roles in the response of other fluvial systems to similar disturbances. Past research (e.g. Rovira *et al.*, 2005a; Rempel and Church, 2009) suggests that river response to mining can vary greatly depending on the fluvial system. Future research needs to test how applicable the conclusions of this study are to other environments, identifying which properties of infilling are universal and what properties are unique to a fluvial system; this will require greater effort to acquire new field datasets.

Conclusions

A comparison of bathymetric surveys indicates that approximately 53% of the initial borrow-pit volume (1·46 million m^3) was infilled with new fluvial sediment over a 2·5 year period of analysis, from May 2010 to October 2012. The pit bed aggraded at a mean rate of 0·88 m yr^{-1} but with an interruption in between January and April 2011, which may have been due to very large fluctuations in reach-scale sediment transport rate promoted by the rising limb of the 2011 flood hydrograph. Extrapolation of the observed infilling trends indicate the borrow pit will infill in 4·4 (using linear regression) to 5·9 (using logarithmic regression) years. The zone of the channel bed experiencing the highest infilling rates was located immediately downstream of the upstream-edge of the borrow pit. This zone translated downstream through time as predicted by existing theory (e.g. van Rijn, 1986).

The results of the Delft3D hydrodynamic numerical modeling indicate that dredging reduced flow velocity in the borrow pit by up to 20% of its pre-dredged value. The magnitude of the reduction in bed stress (R^*) appeared dependent on pit depth (d) and the distance of the borrow-pit bed relative to the upstream-edge of the borrow pit (x_p). The observed spatial distribution of borrow-pit evolution, in terms of both infilling and bed erosion, were significantly correlated with modeled values of R^*. Pit areas with bed stress significantly below the pre-dredged values were more likely to infill, while pit areas with bed stress above the pre-dredged value were more likely to erode.

A reduced-complexity modeling experiment was derived to test if simple metrics of sediment supply and borrow-pit geometry could accurately predict borrow-pit infilling. Over the 2·5 year study period, the model replicated the temporal and spatial patterns of infilling observed in the investigated borrow pit fairly well, estimating that the amount of sand routed into the pit area that became entrapped declined from 11 to 5% during that time. The model also predicted that the pit infilling could be approximately complete after a 10 year period that repeatedly cycled the mean-annual river hydrograph. Results from additional modeling experiments suggest that, for a given borrow-pit volume, deeper borrow pits will infill faster than elongated pit geometries.

Acknowledgements—This study was funded in part by the Louisiana Coastal Protection and Restoration Authority and the Water Institute of the Gulf Science and Engineering Plan. Early versions of this research benefited from counsel by Mark Leadon, Brian Vosberg, Rudy Simoneaux, Denise Reed, and Mike Ramirez. This manuscript benefited from the thoughtful comments of three anonymous reviewers and the associate editor.

References

Alfrink BJ, Van Rijn LC. 1983. Two-equation turbulence model for flow in trenches. *Journal of Hydraulic Engineering* **109**(7): 941–958.

Allison MA, Demas CR, Ebersole BA, Kliess BA, Little CD, Meselhe EA, Powell NJ, Pratt TC, Vosburg BM. 2012. A water and sediment budget for the lower Mississippi–Atchafalaya River in flood years 2008–2010: implications for sediment discharge to the oceans and coastal restoration in Louisiana. *Journal of Hydrology* **432**: 84–97.

Allison MA, Nittrouer JA. 2004. Assessing Quantity and Quality of Sand Available in the Lower Mississippi River Channel for Coastal Marsh and Barrier Island Restoration in Louisiana, Final Technical Report for Subcontract C-162523. Governor's Applied Coastal Research and Development Program: Baton Rouge, LA.

Allison MA, Ramirez MT, Meselhe EA. 2014. Diversion of Mississippi River water downstream of New Orleans, Louisiana, USA to maximize sediment capture and ameliorate coastal land loss. *Water Resources Management* **28**(12): 4113–4126.

Bai Y, Wang Z, Shen H. 2003. Three-dimensional modelling of sediment transport and effects of dredging in the Haihe Estuary. *Estuarine, Coastal and Shelf Science* **56**: 175–186.

Bender CJ, Dean RG. 2003. Wave field modification by bathymetric anomalies and resulting shoreline changes: a review with recent results. *Coastal Engineering* **49**(1): 125–153.

Bijker EW. 1980. Sedimentation in channels and trenches. *Coastal Engineering Proceedings* **1**(17): 1708–1718.

Bird JF. 1980. Geomorphological implications of flood control measures, Lang Lang River, Victoria. *Australian Geographical Studies* **18** (2): 169–183.

Blum MD, Roberts HH. 2009. Drowning of the Mississippi Delta due to insufficient sediment supply and global sea-level rise. *Nature Geoscience* **2**: 488–491.

Boers M. 2005. Effects of a Deep Sand Extraction Pit, Final report of the PUTMOR Measurements at the Lowered Dump Site. Rapport RIKZ/2005.001. RIKZ: The Hague.

Bull WB, Scott KM. 1974. Impact of mining gravel from urban stream beds in the southwestern United States. *Geology* **2**(4): 171–174.

Chang HH. 1987. Modeling fluvial processes in streams with gravel mining. In Sediment Transport in Gravel Bed Rivers, Thorne CR, Bathurst JC, Hey RD (eds). John Wiley & Sons: Chichester; 977–988.

Chen D. 2011. Modeling channel response to instream gravel mining. In Sediment Transport – Flow and Morphological Processes, Bhuiyan F (ed). INTECH: Rijeka.

Chen D, Acharya K, Stone M. 2010. Sensitivity analysis of nonequilibrium adaptation parameters for modeling mining-pit migration. *Journal of Hydraulic Engineering* **136**(10): 806–811.

Chorley RJ. 1962. Geomorphology and General Systems Theory, Geological Survey Professional Paper 500-B. US Government Printing Office: Washington, DC.

Collins BD, Dunne T. 1989. Gravel transport, gravel harvesting, and channel-bed degradation in rivers draining the southern Olympic Mountains, Washington, USA. *Environmental Geology and Water Sciences* **13**(3): 213–224.

Costa J, Schuster R. 1988. Formation and failure of natural dams. *GSA Bulletin* **100**(7): 1054–1068.

Davies DK. 1966. Sedimentary structures and subfacies of a Mississippi River point bar. *The Journal of Geology* **74**(2): 234–239.

Fagerburg TL, Alexander MP. 1994. Underwater Sill Construction for Mitigating Salt Wedge Migration on the Lower Mississippi River, Waterways Experiment Station Report No. WES/MP/HL-94-1. US Army Corps of Engineers, Hydraulics Lab: Vicksburg, MS.

Finkl CW, Khalil SM, Andrews J, Keehn S, Benedet L. 2006. Fluvial sand sources for barrier island restoration in Louisiana: Geotechnical investigations in the Mississippi River. *Journal of Coastal Research* **22**(4): 773–787.

Fredsoe J. 1979. Natural backfilling of pipeline trenches. *Journal of Petroleum Technology* **31**(10): 1–223.

Gaweesh A, Meselhe E. In press. Evaluation of sediment diversion design attributes and their impact on capture efficiency. *Journal of Hydraulic Engineering*. DOI:10.1061/(ASCE)HY.1943-7900.0001114.

Griggs GB, Paris L. 1982. Flood control failure: San Lorenzo River, California. *Environmental Management* **6**(5): 407–419.

González M, Medina R, Espejo A, Tintoré J, Martin D, Orfila A. 2010. Morphodynamic evolution of dredged sandpits. *Journal of Coastal Research* **26**(3): 485–502.

Gouverneur L, Dewals B, Archambeau P, Erpicum S, Pirotton M. 2013. Discussion of "Sensitivity Analysis of Nonequilibrium Adaptation Parameters for Modeling Mining Pit Migration" by Dong Chen, Kumud Acharya, and Mark Stone. *Journal of Hydraulic Engineering* **139**(7): 799–801.

Grant GE, Swanson FJ. 1995. Morphology and processes of valley floors in mountain streams, western Cascades, Oregon. In Natural and Anthropogenic Influences in Fluvial Geomorphology, Costa JE, Miller AJ, Potter KW, Wilcock PR (eds). American Geophysical Union: Washington, DC; 83–101.

Gupta A, Fox H. 1974. Effects of high-magnitude floods on channel form: a case study in Maryland Piedmont. *Water Resources Research* **10**(3): 499–509.

Hajek EA, Edmonds DA. 2014. Is river avulsion style controlled by floodplain morphodynamics? *Geology* **42**(3): 199–202.

Hoitink T. 1997. Morphological Impact of Large Scale Marine Sand Extraction, MScThesis. University of Twente, Enschede.

Hossain S, Eyre BD, McKee LJ. 2004. Impacts of dredging on dry season suspended sediment concentrations in the Brisbane River estuary, Queensland, Australia. *Estuarine, Coastal and Shelf Science* **61**(3): 539–545.

Huang HQ, Nanson GC. 2000. Hydraulic geometry and maximum flow efficiency as products of the principle of least action. *Earth Surface Processes and Landforms* **25**(1): 1–16.

International Association of Dredging Companies and International Association of Ports and Harbors (IADC/IAPH). 2010. Dredging for Development. Opmeer Drokkeril: The Hague.

Jensen JH, Fredsøe J. 2001. Sediment transport and backfilling of trenches in oscillatory flow. *Journal of Waterway, Port, Coastal, and Ocean Engineering* **127**(5): 272–281.

Jensen JH, Madsen ES, Fredsoe J. 1999. Oblique flow over dredged channels. II: Sediment transport and morphology. *Journal of Hydraulic Engineering* **125**(11): 1190–1198.

Jordan PR. 1965. Fluvial Sediment of the Mississippi River t St. Louis, Missouri, US Geological Survey Water-Supply Paper 1802. US Government Printing Office: Washington, DC.

Keller EA, Swanson FJ. 1979. Effects of large organic material on channel form and fluvial processes. *Earth Surface Processes and Landforms* **4**(4): 361–380.

Khalil SM, Finkl CW. 2009. Regional sediment management strategies for coastal restoration in Louisiana, USA. *Journal of Coastal Research, SI* **56**: 1320–1324.

Kirkby MJ. 1976. Maximum sediment efficiency as a criterion for alluvial channels. In River Channel Changes, Gregory KJ (ed). Wiley: New York; 429–442.

Klein M. 1999. Large-scale Sand Pits, MSc Thesis/Report Z2615. Delft Hydraulics, Delft.

Knaapen M, Kelly D. 2012. Lag effects in morphodynamic modelling of engineering impacts. Proceedings, 33rd International Conference on Coastal Engineering (ICCE), Santander, Spain.

Kojima H, Ijima T, Nakamuta T. 1986. Impact of offshore dredging on beaches along the Genkai Sea, Japan. Proceedings, 20th International Conference on Coastal Engineering. American Society of Civil Engineers: Reston, VA; 1281–1295.

Kondolf GM. 1997. PROFILE: hungry water: effects of dams and gravel mining on river channels. *Environmental Management* **21**(4): 533–551.

Kori E, Mathada H. 2012. An assessment of environmental impacts of sand and gravel mining in Nzhelele Valley, Limpopo Province, South Africa. Proceedings, 3rd International Proceedings of Chemical, Biological, and Environmental Engineering; 137–141.

Knuuti K, McComas D. 2003. Assessment of Changes in Channel Morphology and Bed Elevation in Mad River, California, 1971–2000, ERDC/CHL TR-03-16. US Army Engineer Research and Development Center: Vicksburg, MS.

Kraus NC, Larson M. 2001. Mathematical Model for Rapid Estimation of Infilling and Sand Bypassing at Inlet Entrance Channels, ERDC/CHL CHETN-IV-35. US Army Engineer Research and Development Center: Vicksburg, MS.

Kraus NC, Larson M. 2002. Analytical model of navigation channel infilling by cross-channel transport. In Proceedings 28th Coastal Engineering Conference. World Scientific Press: Singapore.

Lane EW. 1955. Design of stable alluvial channels. *Transactions, American Society of Civil Engineers* **2776**(20): 1234–1279.

Langbein WB, Leopold LB. 1964. Quasi-equilibrium states in channel morphology. *American Journal of Science* **262**(6): 782–794.

Langer WH. 2003. A General Overview of the Technology of In-stream Mining of Sand and Gravel Resources, Associated Potential Environmental Impacts, and Methods to Control Potential Impacts, Open-File Report 02-153. US Department of the Interior, US Geological Survey: Reston, VA.

Langer WH, Glanzman VM. 1993. Natural Aggregate: Building America's Future, Circular 1110. US Department of the Interior, US Geological Survey: Denver, CO.

Lapointe MF, Secretan Y, Driscoll SN, Bergeron N, Leclerc M. 1998. Response of the Ha! Ha! River to the flood of July 1996 in the Saguenay region of Quebec: large-scale avulsion in a glaciated valley. *Water Resources Research* **34**(9): 2383–2392.

Lee HY, Fu DT, Song MH. 1993. Migration of rectangular mining pit composed of uniform sediments. *Journal of Hydraulic Engineering* **119**: 64–80.

Legates DR, McCabe GJ, Jr. 1999. Evaluating the use of 'goodness-of-fit' measures in hydrologic and hydroclimatic model validation. *Water Resources Research* **35**(1): 233–241.

Lehre A, Klein R, Jager D. 2009. County of Humboldt extraction review team (CHERT) historical analyses of the Mad River: 2004–2007 update. A County of Humboldt Extraction Review Team report prepared for the Humboldt County board of supervisors. http://www.humboldtgov.org/ArchiveCenter/ [26 August 2015].

Lou X-L, Zeng EY, Ji R-Y, Wang C-P. 2007. Effects of in-channel sand excavation on the hydrology of the Pearl River Delta, China. *Journal of Hydrology* **343**: 230–239.

Marston RA, Bravard J, Green T. 2003. Impacts of reforestation and gravel mining on the Malnant River, Haute-Savoie, French Alps. *Geomorphology* **55**(1): 65–74.

Matsubara Y, Howard AD. 2014. Modeling planform evolution of a mud-dominated meandering river: Quinn River, Nevada, USA. *Earth Surface Processes and Landforms* **39**(10): 1365–1377.

McElroy B, Mohrig D. 2009. Nature of deformation of sandy bedforms. *Journal of Geophysical Research, Earth Surface* **114**(F3): F00A04. DOI: 10.1029/2008JF001220

Meador MR, Layher AO. 1998. Instream sand and gravel mining: environmental issues and regulatory process in the United States. *Fisheries* **23**(11): 6–13.

Meselhe EA, Georgiou I, Allison MA, McCorquodale JA. 2012. Numerical modeling of hydrodynamics and sediment transport in lower Mississippi at a proposed delta building diversion. *Journal of Hydrology* **472**: 340–354.

Meselhe E, Rodrique MD. 2013. Models Performance Assessment Metrics and Uncertainty Analysis. In Report prepared for the Louisiana Coastal Protection and Restoration Authority (CPRA) under the Louisiana Coastal Area (LCA) Mississippi River Hydrodynamics and Delta Management Study. CPRA: Baton Rouge, LA.

Moffatt & Nichol. 2012a. Investigations of Potential Mississippi River Borrow Areas. Final Report. Baton Rouge, LA. http://lacoast.gov/reports/project/4940405~1.pdf (Accessed 22 August 2014)

Moffatt & Nichol. 2012b. Mississippi River Long Distance Sediment Pipeline, Final (95%) Design Report. Baton Rouge, LA.

Morris GL, Annandale G, Hotchkiss R. 2008. Reservoir sedimentation. In Sedimentation Engineering Process Measurements, Modeling and Practices, Garcia M (ed). American Society of Civil Engineers: Reston, VA.

Morris GL, Fan J. 1997. Reservoir Sedimentation Handbook: Design and Management of Dams, Reservoir, and Watersheds for Sustainable Use. McGraw Hill: New York.

Mossa J, McLean M. 1997. Channel planform and land cover changes on a mined river floodplain: Amite River, Louisiana, USA. *Applied Geography* **17**(1): 43–54.

Murray AB. 2007. Reducing model complexity for explanation and prediction. *Geomorphology* **90**(3): 178–191.

Neyshabouri SAAS, Farhadzadeh A, Amini A. 2002. Experimental and field study on mining-pit migration. *International Journal of Sediment Research* **17**(4): 323–331.

Nicholas AP. 2010. Reduced-complexity modeling of free bar morphodynamics in alluvial channels. *Journal of Geophysical Research, Earth Surface* **115**(F4): F04021. DOI:10.1029/2010JF001774.

Nittrouer JA, Allison MA, Campanella R. 2008. Bedform transport rates for the lowermost Mississippi River. *Journal of Geophysical Research, Earth Surface* **113**(F3): F03004. DOI. 10.1029/2007JF000795

Nittrouer JA, Viparelli E. 2014. Sand as a stable and sustainable resource for nourishing the Mississippi River delta. *Nature Geoscience* **7**(5): 350–354.

Ohimain EI. 2004. Environmental impacts of dredging in the Niger Delta. *Terra et Aqua* **97**: 9–19.

Owen MR, Pavlowsky RT, Martin DJ. 2012. Big River Borrow Pit Monitoring Project. Ozarks Environmental and Water Resources Institute, Missouri State University: Springfield, MO.

Padmalal D, Maya K, Sreebha S, Sreeja R. 2008. Environmental effects of river sand mining: a case from the river catchments of Vembanad Lake, Southwest coast of India. *Environmental Geology* **54**(4): 879–889.

Petit F, Poinsart D, Bravard J-P. 1996. Channel incision, gravel mining and bed load transport in the Rhône River upstream of Lyon, France ('canal de Miribel'). *Catena* **26**(3): 209–226.

Peyronnin N, Green M, Parsons CR, Owens A, Reed D, Chamberlain J, Groves DG, Rhinehart WK, Belhadjali K. 2013. Louisiana's 2012 coastal master plan: overview of a science-based and publicly informed decision-making process. *Journal of Coastal Research* **67**(sp1): 1–15.

Phillips BC, Sutherland AJ. 1989. Spatial lag effects in bed load sediment transport. *Journal of Hydraulic Research* **27**(1): 115–133.

Phillips JD. 2003. Sources of nonlinearity and complexity in geomorphic systems. *Progress in Physical Geography* **27**(1): 1–23.

Ponce VM, Simons DB, Garcia JL. 1979. Modeling alluvial channel bed transients. *Journal of the Hydraulics Division* **105**(3): 245–256.

Poulin R, Pakalnis RC, Sinding K. 1994. Aggregate resources: production and environmental constraints. *Environmental Geology* **23**(3): 221–227.

Ramirez MT, Allison MA. 2013. Suspension of bed material over sand bars in the Lower Mississippi River and its implications for Mississippi delta environmental restoration. *Journal of Geophysical Research, Earth Surface* **118**(2): 1085–1104. DOI:10.1002/jgrf.20075.

Ray PK. 1979. Structure and sedimentological history of the overbank deposits of a Mississippi River point bar. *Journal of Sedimentary Research* **46**(4): 788–801. DOI:10.1306/212F7059-2B24-11D7-8648000102C1865D.

Rempel LL, Church M. 2009. Physical and ecological response to disturbance by gravel mining in a large alluvial river. *Canadian Journal of Fisheries and Aquatic Sciences* **66**(1): 52–71.

Richardi DC, Hopkins P, Boshart WM. 2013. Monitoring Plan for Mississippi River Sediment Delivery System – Bayou Dupont (BA-39). State of Louisiana, Coastal Protection and Restoration Authority, July 2013. http://coastal.la.gov/resources/library/ [2 June 2014].

Rinaldi M, Simon A. 1998. Bed-level adjustments in the Arno River, central Italy. *Geomorphology* **22**(1): 57–71.

Roos PC, Hulscher SJ, de Vriend HJ. 2008. Modelling the morphodynamic impact of offshore sandpit geometries. *Coastal Engineering* **55**(9): 704–715.

Rovira A, Batalla RJ, Sala M. 2005a. Response of a river sediment budget after historical gravel mining (The lower Tordera, NE Spain). *River Research and Applications* **21**(7): 829–847.

Rovira A, Batalla RJ, Sala M. 2005b. Fluvial sediment budget of a Mediterranean river: the lower Tordera (Catalan Coastal Ranges, NE Spain). *Catena* **60**(1): 19–42.

Saloman CH, Naughton SP, Taylor JL. 1982. Benthic Community Response to Dredging Borrow Pits, Panama City Beach, Florida. Miscellaneous Report No. 82-3. US Army Corps of Engineers Coastal Engineering Research Center: Fort Belvoir, VA.

Simon A. 1989. A model of channel response in disturbed alluvial channels. *Earth Surface Processes and Landforms* **14**(1): 11–26.

Simon A. 1992. Energy, time, and channel evolution in catastrophically disturbed fluvial systems. *Geomorphology* **5**(3): 345–372.

Smith DG, Pearce CM. 2002. Ice jam-caused fluvial gullies and scour holes on northern river flood plains. *Geomorphology* **42**(1): 85–95.

US Army Corps of Engineers (USACE). 2015. The U.S. Water System – Transportation Facts and Information. Navigation and Civil Works Decision Support Center: Alexandria, VA.

Van Dijk WM, Schuurman F, vab de Lagaweg WI, Kleinhans MG. 2014. Bifurcation instability and chute cutoff development in meandering gravel-bed rivers. *Geomorphology* **213**: 277–291.

Van Lancker VRM, Bonne WM, Garel E, Degrendele K, Roche M, Van den Eynde D, Bellec VK, Brière C, Collins MB, Velegrakis AF. 2010. Recommendations for the sustainable exploitation of tidal sandbanks. *Journal of Coastal Research, SI* **51**: 151–164.

Van Rijn LC. 1984a. Sediment transport, part I: bed load transport. *Journal of Hydraulic Engineering* **110**(10): 1431–1456.

Van Rijn LC. 1984b. Sediment transport, part II: suspended load transport. *Journal of Hydraulic Engineering* **110**(11): 1613–1641.

Van Rijn LC. 1986. Sedimentation of dredged channels by currents and waves. *Journal of Waterway, Port, Coastal, and Ocean Engineering* **112**(5): 541–559.

Van Rijn LC, Tan GL. 1985. SUTRENCH-model, Two-dimensional Vertical Mathematical Model for Sedimentation in Dredged Channels and Trenches by Currents and Waves. Rijkswaterstaat Communications: The Hague.

Van Rijn LC, Walstra DJR. 2002. Morphology of Pits, Channels, and Trenches, Report prepared for DG RijksWaterstaat Rijks-Instituut voor Kust en Zee. RIKZ: The Hague.

Walstra DJR, Van Rijn LC, Aarninkhof S. 1998. Sand Transport at the Middle and Lower Shoreface of the Dutch Coast; Simulations of SUTRENCH-model and Proposal for Large-scale Laboratory Tests, Report Z2378. Delft Hydraulics: Delft.

Walstra DJR, Van Rijn LC, Hoogewoning SE, Aarninkhof SGJ. 1999. Morphodynamic modelling of dredged trenches and channels. In

Coastal Sediments. American Society of Civil Engineers: Reston, VA; 2355–2370.

Watson CC, Biedenharn DS, Scott SH. 1999. Channel Rehabilitation: Processes, Design, and Implementation. US Army Engineering Research and Development Center:: Vicksburg, MS.

Wishart D, Warburton J, Bracken L. 2008. Gravel extraction and planform change in a wandering gravel-bed river: The River Wear, Northern England. *Geomorphology* **94**(1): 131–152.

Yang CT. 1976. Minimum unit stream power and fluvial hydraulics. *Journal of the Hydraulics Division* **102**(7): 919–934.

Supporting Information

Additional supporting information may be found in the online version of this article at the publisher's web site.